CHIN. PHYS. LETT. Vol. 34, No. 6 (2017) 062501

# Elliptic Flow Splitting between Particles and their Antiparticles in Au+Au Collisions from a Multiphase Transport Model *

Zhen-Yu Xu(徐振宇), Jian-Li Liu(刘剑利), Pan-Pan Zhang(张盼盼), Jing-Bo Zhang(张景波), Lei Huo(霍雷)**
*Department of Physics, Harbin Institute of Technology, Harbin 150001*

(Received 20 January 2017)

*The elliptic flow $v_2$, for $\pi^{\pm}$, $K^{\pm}$, $p$ and $\bar{p}$ in Au+Au collisions at center-of-mass energies $\sqrt{s_{\rm NN}}$ = 7.7, 11.5, 14.5 and 19.6 GeV, is analyzed using a multiphase transport model. A significant difference in the $v_2$ values for $p$ and $\bar{p}$ is observed, and the values of $v_2$ splitting are larger compared with $\pi^+$ and $\pi^-$, $K^+$ and $K^-$. The difference increases with decreasing the center-of-mass energy. The effect of the quark coalescence mechanism in a multi-phase transport model to the value of elliptic difference $\Delta v_2$ between $p$ and $\bar{p}$ has been discussed. The simulation of Au+Au collisions at 14.5 GeV shows that the effect of hadron cascade to $\Delta v_2$ is not obvious, and a larger parton-scattering cross section can lead to a larger $\Delta v_2$.*

*PACS:* 25.75.Ld, 25.75.−q, 25.75.Nq DOI: 10.1088/0256-307X/34/6/062501

One of the main purposes of heavy ion programs at facilities like the relativistic heavy ion collider (RHIC) and the large hadron collider (LHC) is to characterize the hot and dense matter that consists of deconfined quarks and gluons which are produced in the initial stage of high-energy heavy ion collisions. Researchers use the quark-gluon plasma (QGP) to describe the states of deconfined matter. To understand the formation of the QGP and to study the structure of quantum chromodynamics (QCD) diagram, the beam energy scan (BES) program was started at RHIC.[1] In the years of 2010 and 2011, the Au+Au collisions at $\sqrt{s_{\rm NN}}$ = 7.7, 11.5, 19.6, 27, 39 and 62.4 GeV were recorded in the solenoidal tracker at experiment RHIC (STAR), and the data of 14.5 GeV was recorded in the year of 2014.

The elliptic flow ($v_2 = \langle\cos[2(\varphi - \Psi_{\rm RP})]\rangle$, where $\varphi$ is the azimuthal angle of the particle momentum, and $\Psi_{\rm RP}$ is the azimuth of the reaction plane) is one of the most widely studied observables in non-central collisions of high-energy heavy ion physics.[2] It is used to describe the shape conversion from the almond overlapped region into azimuthal anisotropy in the momentum space.[3] With the experimental data of 200 GeV Au+Au collisions, a mass ordering of $v_2$ was observed at low transverse momentum ($p_{\rm T} < 2\,{\rm GeV}/c$),[4−6] and at intermediate transverse momentum ($2 < p_{\rm T} < 6\,{\rm GeV}/c$), a number-of-constituent quark (NCQ) scaling of $v_2$ was observed for the identified hadrons.[7,8] The observation of NCQ scaling means that at top RHIC energy, a deconfined system was formed.[9,10] In the BES program, a beam-energy-dependent value of elliptic flow difference $\Delta v_2$ between particles and their corresponding antiparticles was observed, and the difference increases with decreasing the center-of-mass energy.[11,12] This result indicates that, at lower energies, particles and antiparticles are not consistent with the universal NCQ scaling which was observed at $\sqrt{s_{\rm NN}}$ = 200 GeV. There are several theoretical works that have tried to explain this experimental result.[13−16] In particular, Dunlop *et al.*[13] studied the elliptic flow of transported and produced quarks. For the existence of baryon stop, net baryon density in heavy ion collisions is larger at lower collision energies. The transport quarks may have experienced more scatterings for the fact that they have been transported over a significant rapidity range. Thus the transported quarks will obtain larger $v_2$ because they are closer to the thermal limit, and the $v_2$ splitting of particles and antiparticles may be due to the difference between the evolution processes of the quarks.

In this Letter, we use a multi-phase transport (AMPT) model to analyze the beam energy and the transverse momentum ($p_{\rm T}$) dependence of the elliptic flow $v_2$. The effect of quark coalescence mechanism to the elliptic flow difference $\Delta v_2$ of proton and antiproton are analyzed. The effect of parton cascade and hadron cascade on the elliptic flow difference of the proton and antiproton are also discussed.

The AMPT model is designed for high-energy heavy ion collisions.[17] There are two versions of it: the default AMPT model and the string melting AMPT model, and both of these versions use the heavy ion jet interaction generator (HIJING)[18] to generate their initial conditions. In our study, we use the string melting version to reproduce the elliptic flow with different energies and different parton-scattering cross sections. In the initial stage, the hadrons produced in the AMPT model with string melting are converted to quarks and antiquarks, and Zhang's parton cascade (ZPC)[19] is used to describe the partonic interactions with the differential parton-scattering cross section

$$\frac{d\sigma}{dt} = \frac{9\pi\alpha_{\rm s}^2}{2\mu^2}, \tag{1}$$

*Supported by the National Natural Science Foundation of China under Grant No U1332125, and the Program for Innovation Research of Science in Harbin Institute of Technology under Grant No B201408.
**Corresponding author. Email: lhuo@hit.edu.cn
© 2017 Chinese Physical Society and IOP Publishing Ltd

where $\alpha_s$ is the strong coupling constant, and $\mu$ is the screening mass in the partonic matter. We can control the value of the screening mass to obtain a specified cross section. At the end of the partonic evolution, quarks and antiquarks are recombined to form hadrons through a simple quark coalescence model for the scenario of string melting, and a relativistic transport (ART) model[20] is used to treat hadron scatterings.

In this study, some default parameters are used in the string melting version of the AMPT model. The values of $a = 2.2$ and $b = 0.5\,\mathrm{GeV}^{-2}$ are chosen in HIJING for the Lund string fragmentation function. Also, the values $\alpha_s = 0.47$ and $\mu = 4.56$, 3.23 or $2.28\,\mathrm{fm}^{-1}$ corresponding to a total parton-scattering cross section of 1.5, 3 or 6 mb are used. The value of $v_2$ is calculated corresponding to the reaction plane, i.e., the real plane which was spanned by the impact parameter vector and the beam direction.

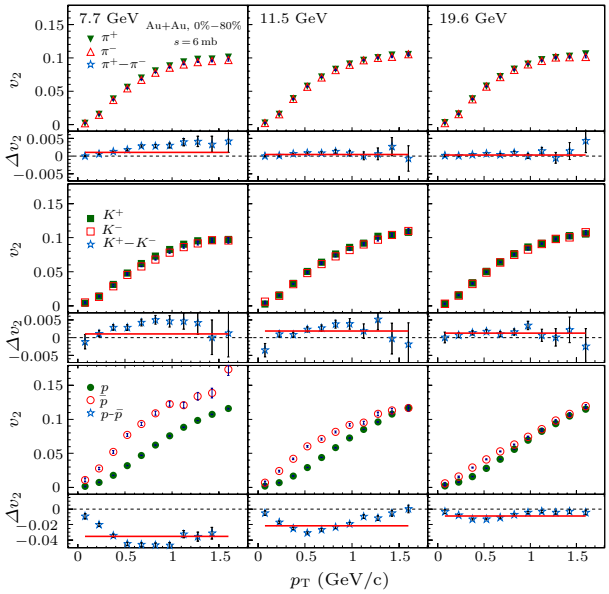


**Fig. 1.** (Color online) The elliptic flow $v_2$, of $\pi^+$, $\pi^-$, $K^+$, $K^-$, $p$ and $\bar{p}$ as a function of the transverse momentum $p_T$, for 0%–80% central Au+Au collisions from the AMPT model with a parton-scattering cross section of 6 mb. The statistic uncertainties are shown by vertical lines. The bottom row of each panel shows the difference between a particle and corresponding antiparticle $v_2(p_T)$ and a fit with a horizontal line to make a clear comparison.

We calculate the elliptic flow for $\pi^+$, $\pi^-$, $K^+$, $K^-$, $p$ and $\bar{p}$ as a function of the transverse momentum $p_T$, for 0%–80% central Au+Au collisions, and the results are shown in Fig. 1. In the lower rows of each panel in Fig. 1, the elliptic flow difference $\Delta v_2$ between particles and their corresponding antiparticles is shown, and the red line shows a horizontal fit to $\Delta v_2$. The statistical uncertainties are described by vertical lines, as we can see, some of them are smaller than the symbol size. At lower energies, an increasing difference between $v_2(\pi^+)$ and $v_2(\pi^-)$ is observed at STAR,[12] where $v_2(\pi^-)$ is larger than $v_2(\pi^+)$ for all $p_T$ values. This phenomenon may be attributable to the mean-field potentials in the hadronic stage.[14] Probably because the present AMPT model does not include this process, we cannot see an obvious difference between $v_2(\pi^+)$ and $v_2(\pi^-)$ in the simulation. The $v_2(p_T)$ values of $K^+$ are larger compared with $K^-$, but the $v_2$ difference of $K^+$ and $K^-$ is not obvious.

In contrast to $K^\pm$ and $\pi^\pm$, a significant difference of $v_2$ between $p$ and $\bar{p}$ is observed. The elliptic flow difference $\Delta v_2$ of $p$ and $\bar{p}$ increases with decreasing the beam energy, and the values of $\Delta v_2$ are consistent with the results in Fig. 22 of Ref. [12]. It is noteworthy that the result of AMPT simulations cannot reproduce the experimental results from the STAR collaboration, where the proton, compared with the antiproton, shows a significantly larger $v_2$.[12] The $v_2$ difference between particles and antiparticles at higher energies ($E > 19.6$ GeV) are very small in the AMPT model, thus we do not show the results for these higher energy collisions here.

If the reconstructed event plane is used in the analysis, the value of elliptic flow $v_2$ will be changed. We use the $\eta$-sub event method to reconstruct the event plane event-by-event and to calculate the elliptic flow of (anti)particles. The event plane was reconstructed using the procedure described in Ref. [21]. The results show that the values of elliptic flow for particles and antiparticles are larger than that corresponding to the real event plan in the model. However, the values of $v_2$ splitting between particles and their corresponding antiparticles from the $\eta$-sub event method are very close to the results from the real plane. We will use the real plane in the following.

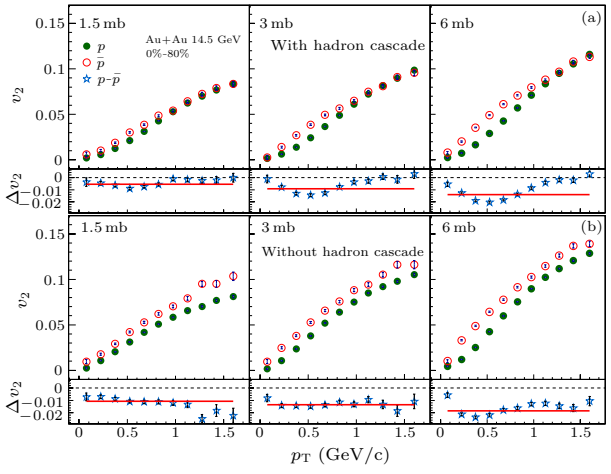


**Fig. 2.** (Color online) The elliptic flow $v_2$ of $p$ and $\bar{p}$ as a function of the transverse momentum $p_T$ for 0%–80% central Au+Au collisions from the string melting version of the AMPT model: (a) with hadron cascade and (b) without hadron cascade. The statistic uncertainties are shown by vertical lines. The bottom row of each panel shows the difference between a particle and corresponding antiparticle $v_2(p_T)$ and a fit with a horizontal line to make the comparison clear.

The partonic evolution plays an important role in collectivity. The elliptic flow $v_2$ was excepted to develop at the stage of partonic.[22,23] To study the influ-

ence of parton cascade on elliptic flow difference $\Delta v_2$, we set the parton-scattering cross section to 1.5 mb, 3 mb and 6 mb, respectively, in the string melting version of the AMPT model. Figure 2 shows the result of elliptic flow for $p$ and $\bar{p}$ with the centrality range of 0%–80% events. Elliptic flow of charged pions and charged kaons are not shown in Fig. 2 for their elliptic flow difference $\Delta v_2$ between particle and antiparticle are really small at all these three parton-scattering cross sections. In Fig. 2, we can see that the elliptic flow difference $\Delta v_2$ between $p$ and $\bar{p}$ shows a parton-scattering cross section dependence, the value of $\Delta v_2$ increases with the parton-scattering cross section.

In the AMPT model, hadron cascade is based on the ART model which includes baryon–baryon, baryon–meson, and meson–meson elastic, as well as inelastic, scatterings.[17] In Fig. 2, we also show the elliptic flow of $p$ and $\bar{p}$ from the AMPT model without hadron cascade. It can be seen that the elliptic flow of $\bar{p}$ becomes smaller for the thermalization process in hadron cascade. The $v_2$ difference between $p$ and $\bar{p}$ becomes smaller when hadron cascade is included, but the decrease of $\Delta v_2$ is not obvious.

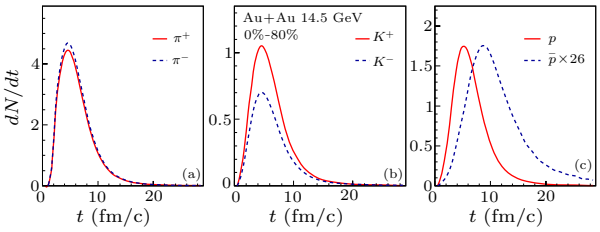


**Fig. 3.** (Color online) Formation time distribution of $\pi^+$, $\pi^-$, $K^+$, $K^-$, $p$ and $\bar{p}$ for 0%–80% central Au+Au collisions at $\sqrt{s_{\rm NN}} = 14.5$ GeV from the string melting version of the AMPT model. Solid lines represent particles and dashed lines for antiparticles. Because the number of $\bar{p}$ is less than $p$ at these energies, the distribution of $\bar{p}$ is multiplied by a number to make the comparison more obvious.

In the string melting version of the AMPT model, (anti)quarks freeze out after completing their last scatterings, then recombine to form hadrons in the coordinate space. The elliptic flow of a hadron will be affected by the space momentum correlation of a quark and antiquark.[24] Quark coalescence follows the 'proximity principle', that is, two (or three) quarks nearest in the coordinate space form a hadron. At lower collision energies, a part of the quarks in the nucleus are transported to midrapidity due to the existence of baryon stop,[13] i.e., a baryon-rich system is formed. In Fig. 3, we show the distribution of formation time of $\pi^+$, $\pi^-$, $K^+$, $K^-$, $p$ and $\bar{p}$ for 0%–80% central Au+Au collisions at $\sqrt{s_{\rm NN}} = 14.5$ GeV. Owing to the quark coalescence mechanism in the AMPT model, it can be seen from Figs. 3(a)–3(c) that the formation time for mesons and their corresponding antiparticles ($\pi^\pm$ and $K^\pm$) is almost the same, and the average formation time of $p$ is earlier than $\bar{p}$.

It is worth noting that the formation time of hadrons are defined as the latest time of constituent quarks plus additional 0.7 fm/$c$ in its rest frame, thus we analyze the freeze out time of constituent quarks of $\pi^\pm$, $K^\pm$, $p$ and $\bar{p}$ at $\sqrt{s_{\rm NN}} = 7.7$, 11.5, 14.5 and 19.6 GeV. We find that the freeze out time of quark and antiquark which form $\pi^\pm$ (or $K^\pm$) is almost the same at all these four energies. The average freeze out time of constituent quarks of $\bar{p}$ is later than $p$, as shown in Fig. 4. In Fig. 4 we can also see that the freeze out time of $\bar{u}$ becomes late with decreasing the beam energy.

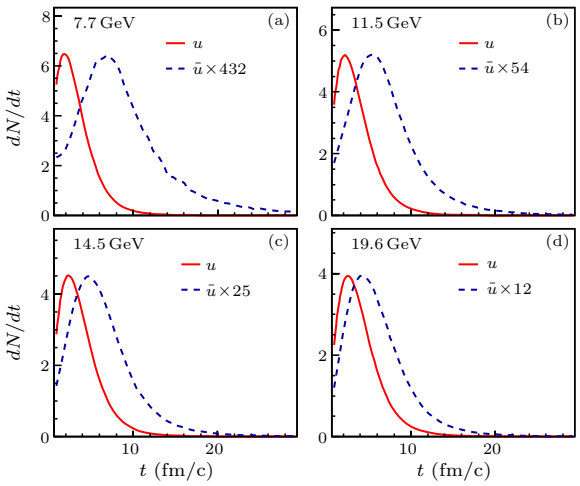


**Fig. 4.** (Color online) Freeze out time distribution of constituent quarks $u$ and $\bar{u}$ of (anti)proton at $\sqrt{s_{\rm NN}} = 7.7$–19.6 GeV. Solid lines represent quark and dashed lines for antiquark. Because the number of $\bar{u}$ is less than $u$ at these energies, the distribution of $\bar{u}$ is multiplied by a number to make the comparison more obvious.

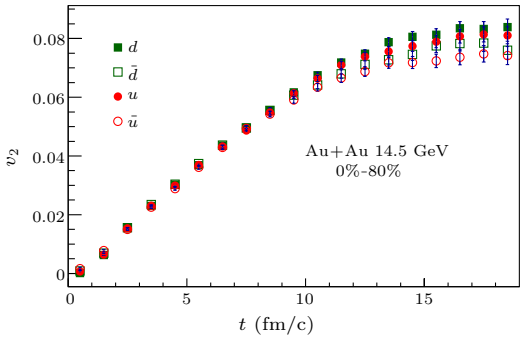


**Fig. 5.** (Color online) Time evolution of integrated elliptic flow of quarks which form midrapidity hadrons for 0%–80% central Au+Au collisions from the string melting version of the AMPT model. The statistic uncertainties are shown by the vertical lines.

The time evolution of the integrated elliptic flow of constituent quarks which form midrapidity hadrons is shown in Fig. 5. In Fig. 5, (anti)quarks are included in the calculation until they recombined to form hadrons. It can be seen that $v_2$ of (anti)quarks is increasing till about 15 fm/$c$. The freeze out time of quark and antiquark which form $\pi^\pm$ (or $K^\pm$) is almost the same. This is consistent with the results shown in Fig. 1 that the $v_2$ difference for mesons is almost close to zero. For $p$ and $\bar{p}$, the average freeze out time of their constituent quarks $u$ is earlier than $\bar{u}$. This implies that $v_2$ of constituent quarks which form $\bar{p}$ is larger than

that of $p$. We calculate the differential elliptic flow $v_2$ of constituent quarks which form proton and antiproton at $\sqrt{s_{\rm NN}} = 14.5\,{\rm GeV}$, and the results are shown in Fig. 6. It can be seen that the value of $v_2$ of antiquarks is obviously larger than quarks. For charged pions, the $v_2$ difference of the corresponding constituent quark and antiquark is really small (not shown). The case of charged kaons is similar to charged pions.

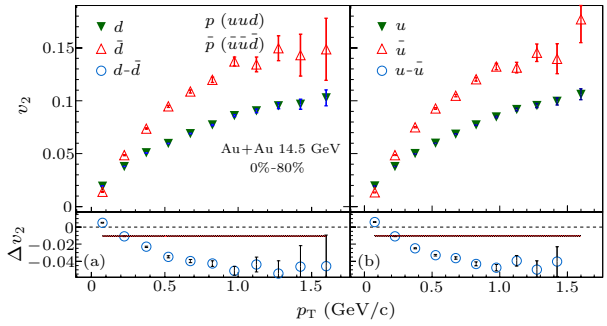


**Fig. 6.** (Color online) The elliptic flow of constituent quarks of $p(uud)$ and $\bar{p}(\bar{u}\bar{u}\bar{d})$ as a function of the transverse momentum $p_{\rm T}$. The statistic uncertainties are shown by the vertical lines. The bottom row of each panel shows the difference between quarks and antiquarks $v_2(p_{\rm T})$ and a fit with a horizontal line to make the comparison clear.

In summary, we have studied the elliptic flow $v_2$ and the elliptic flow difference $\Delta v_2$ of $\pi^+$, $K^+$, $p$ and their antiparticles in Au+Au collisions at $\sqrt{s_{\rm NN}} = 7.7$, 11.5, 14.5 and 19.6 GeV by using the AMPT model. At the energies of 7.7, 11.5, and 14.5 GeV, a significant elliptic flow difference $\Delta v_2$ between $\bar{p}$ and $p$ is obtained, and the value of $\Delta v_2$ increases with decreasing the beam energy. The effect of parton cascade and hadron cascade to the elliptic flow difference of $\bar{p}$ and $p$ has been studied. The result shows that the value of $\Delta v_2$ increases with the parton-scattering cross section, and hadron cascade makes the elliptic flow difference decrease slightly. Our analysis shows that the quark coalescence mechanism in the AMPT model can lead to larger elliptic flow $v_2$ of $\bar{p}$ than $p$ at lower collision energies in the beam-energy scan program at RHIC. This means that $v_2$ and $\Delta v_2$ may be affected by the process of quark coalescence.

## References


[1] Aggarwal M M, Ahammed Z, Alakhverdyants A V et al 2010 arXiv:1007.2613[nucl-ex]
[2] Voloshin S and Zhang Y 1996 *Z. Phys.* C **70** 665
[3] Poskanzer A M and Voloshin S A 1998 *Phys. Rev.* C **58** 1671
[4] Adler C, Ahammed Z, Allgower C et al 2001 *Phys. Rev. Lett.* **87** 182301
[5] Adams J, Adler C, Aggarwal M M et al 2004 *Phys. Rev. Lett.* **92** 052302
[6] Adams J, Aggarwal M M, Ahammed Z et al 2005 *Phys. Rev. Lett.* **95** 122301
[7] Voloshin S A, Poskanzer A M and Snellings R 2008 arXiv:0809.2949[nucl-ex]
[8] Abelev B I, Aggarwal M M, Ahammed Z et al 2007 *Phys. Rev.* C **75** 054906
[9] Abelev B I, Aggarwal M M, Ahammed Z et al 2010 *Phys. Rev.* C **81** 044902
[10] Abelev B I, Aggarwal M M, Ahammed Z et al 2007 *Phys. Rev. Lett.* **99** 112301
[11] Adamczyk L, Adkins J K, Agakishiev G et al 2013 *Phys. Rev. Lett.* **110** 142301
[12] Adamczyk L, Adkins J K, Agakishiev G et al 2013 *Phys. Rev.* C **88** 014902
[13] Dunlop J C, Lisa M A and Sorensen P 2011 *Phys. Rev.* C **84** 044914
[14] Xu J, Chen L W, Ko C M et al 2012 *Phys. Rev.* C **85** 041901
[15] Steinheimer J, Koch V and Bleicher M 2012 *Phys. Rev.* C **86** 044903
[16] Ko C M, Song T, Li F et al 2014 *Nucl. Phys.* A **928** 234
[17] Lin Z W, Ko C M, Li B A et al 2005 *Phys. Rev.* C **72** 064901
[18] Wang X N and Gyulassy M 1991 *Phys. Rev.* D **44** 3501
[19] Zhang B 1998 *Comput. Phys. Commun.* **109** 193
[20] Li B A and Ko C M 1995 *Phys. Rev.* C **52** 2037
[21] Sun X, Liu J L, Schmah A et al 2015 *J. Phys.* G **42** 115101
[22] Tian J, Chen J H, Ma Y G et al 2009 *Phys. Rev.* C **79** 067901
[23] Li N and Shi S S 2011 *Chin. Phys. Lett.* **28** 122502
[24] Liu J L, Shan L Q, Feng Q C et al 2009 *Chin. Phys. Lett.* **26** 072501